Synthesis and cellular uptake of porphyrin decorated iron oxide nanoparticles—a potential candidate for bimodal anticancer therapy†

Hongwei Gu,[a] Keming Xu,[b] Zhimou Yang,[a] Chi K. Chang[a] and Bing Xu*[ab]

Received (in Cambridge, UK) 2nd June 2005, Accepted 16th June 2005
First published as an Advance Article on the web 14th July 2005
DOI: 10.1039/b507779f

This paper reports the synthesis, characterization, and cellular uptake of the conjugate of porphyrin and iron oxide nanoparticles, which may lead to a bimodal anticancer agent that can be used in the combinational treatment of photodynamic therapy (PDT) and hyperthermia therapy (HT).

Cancer, the uncontrolled growth and spread of malignant cells that can affect almost any tissue of the body, remains a major burden to human health. While the major research activities of chemotherapy have focused on research and development of new therapeutic drugs directed against specific targets in cancer cells,[1] substantial efforts have also been devoted to improve minimal or non-invasive treatment methods against cancer. Among the non-invasive protocols, hyperthermia (HT)[2–4] and photodynamic therapy (PDT)[5–7] are receiving renewed interests because of the recent advances in the chemistry of photosensitizers[6] and the demonstration of HT by AC magnetic field-induced excitation of superparamagnetic nanoparticles.[3] Since HT can increase the cellular uptake of oxygen molecules,[2] which are crucial for PDT,[6] and the preferential uptake of porphyrin derivatives in tumors[6] may help localize the magnetic nanoparticles in tumors for an HT protocol, it is logical to combine these two modalities to maximize the efficiency of the treatment of cancer. To construct a molecular conjugate of porphyrin derivatives (*i.e.*, the photosensitizers) and the nanoparticles of iron oxides (*e.g.*, magnetite) as the bimodal agents for PDT and HT, we chose porphyrin derivatives and magnetite as the building blocks because (i) both porphyrin derivatives and iron oxides are biocompatible; (ii) biological processes allow both iron oxides and porphyrin derivatives to be biodegradable after treatment; (iii) the well-studied pharmacokinetics and low systemic toxicity have already led to some clinical trials and usage of porphyrin derivatives in PDT and iron oxides in HT;[3,6] and (iv) porphyrin derivatives and iron oxides are complementary in both properties and functions.

In order to form stable covalent bonds between the porphyrin derivatives and iron oxide nanoparticles, we choose dopamine as the molecular anchor because its dihydroxybenzene part binds tightly to the surface of metal oxides (including iron oxide) *via* M–O bonds.[8,9] Moreover, the exceptional thermal stability of the dopamine-based anchor on the iron oxide surfaces[9] satisfies the requirement of HT. We choose magnetite as the superparamagnetic material because a recently developed synthetic procedure offers a convenient means to control the sizes and shapes of the magnetite nanoparticles from 6 to 50 nm in a relatively precise manner,[10,11] which should facilitate the search for the optimal sizes of the nanoparticles for HT applications. We choose **3** as the porphyrin derivative[12] with which to develop the synthetic route because **3** is readily available and bears two amino groups for functionalization. Using these simple starting materials, we obtained a stable conjugate of porphyrin and magnetite nanoparticles in four steps with an overall yield of 60%. This work not only offers a method to obtain large amounts of the desired conjugate, but also meets the most important challenge for HT, that is, to develop versatile and robust surface chemistry to functionalize superparamagnetic nanoparticles.[3]

Scheme 1 illustrates the synthetic pathway for making the conjugate Fe_3O_4-porphyrin nanoparticles (**5**). After an *N*-hydroxysuccinimide (NHS) activated derivative of dopamine (**1**) reacted with the diaminoporphyrin (**3**), a simple deprotection to remove the benzyl groups afforded **4** in good yield (65%). Reacting **4** (5 mg, in 2 mL of MeOH/$CHCl_3$ = 1:1) with magnetite nanoparticles[10] (30 mg, in 5 mL of hexane) in a ultrasonic bath for 60 minutes gave a red-brown mixture, which was centrifuged and re-dissolved in methanol. After washing the methanol solution three times using chloroform, high-speed centrifugation (12000 rpm) afforded the final product **5**.

We first used transmission electron microscopy (TEM) to compare the morphologies of the as-prepared magnetite and **5**. TEM indicated a narrow size distribution (less than 5%) of the magnetite nanoparticles made by using the procedures of Sun *et al.*[10] Selected area electron diffraction (SAED) patterns also showed that the nanoparticles are highly crystalline; the

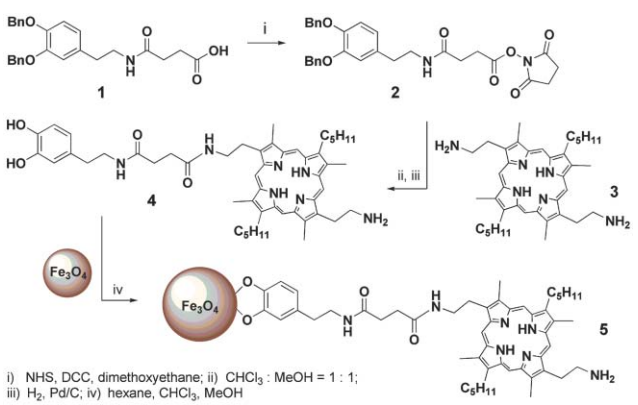

Scheme 1 Synthesis of Fe_3O_4-porphyrin (**5**).

[a]*Department of Chemistry, The Hong Kong University of Science & Technology, Clear Water Bay, Hong Kong, China. E-mail: chbingxu@ust.hk; Fax: +852 2358 1594; Tel: +852 2358 7351*
[b]*Bioengineering program, The Hong Kong University of Science & Technology, Clear Water Bay, Hong Kong, China*
† Electronic supplementary information (ESI) available: synthesis of **4**; EDP, XPS, ToF-SIMS and magnetic measurement of the conjugate (**5**). See http://dx.doi.org/10.1039/b507779f

diffraction rings match the crystal planes of magnetite ({220}, {311}, {400}, {422,}, {511} and {440}, Fig. 1A, inset), which was further demonstrated by high resolution TEM (Fig. 1C). Although the nanoparticles of **5** slightly aggregate due to the less hydrophilic porphyrin molecules that are anchored on the surface of the magnetite, the TEM image of **5** (Fig. 1B) indicates that the morphology of these nanoparticles changes little. The high-resolution TEM (HRTEM) image of **5** (Fig. 1D) also indicates that the crystallinity of the nanoparticles is retained very well, which assures that the reactions between the dihydroxybenzene linkers and the surfaces of magnetite nanoparticles do not drastically alter the magnetic properties of the nanoparticles. Magnetic measurement (ESI†) on a SQUID magnetometer indicates that the nanoparticles of **5** are superparamagnetic at room temperature. The X-ray photoelectron spectrum (XPS) of **5** shows peaks at 712.0 and 726.1 eV (Fe2p), corresponding to the binding energies of iron in an FeO environment (ESI†). The time-of-flight secondary ion mass spectrum (ToF-SIMS) of **5** displays a mass peak at m/z = 177 ($FeO_2C_7H_5^+$), proving that the dihydroxybenzene group covalently anchors on the surface of **5** (ESI†).

In addition to the characteristic Q-band of porphyrin at 500–620 nm, the UV-vis spectrum of the methanol solution of **5** exhibits two absorption maxima, 280 nm and 400 nm. The former originates from the phenyl group, and the latter belongs to the Soret band of porphyrin. These peaks are similar to the absorption spectra of the methanol solution of **4**, indicating the presence of **4** on the magnetite nanoparticles (Fig. 2A). Being excited at the wavelength of 400 nm, **5** exhibits two strong emission peaks located at 580 and 632 nm, which are shifted significantly to the blue region compared with the emission spectrum of **4** (λ_{em} = 625 and 690 nm). The blue shift in the emission spectrum of **5** also agrees with the increase of the baseline toward the blue in the absorption spectrum of **5**, which may result from a splitting of the Soret band buried underneath.[13] These blue shifts suggest that these surface-anchored porphyrin moieties might form π–π dimers whose porphyrin units exhibit stronger interaction for the *y*-polarized transition dipoles.[13] The bright-red fluorescent image of **5** (inset, Fig. 2B) further demonstrates the existence of porphyrin on the surface of the nanoparticles of **5**. The fluorescence of **5** proves that the presence of superparamagnetic nanoparticles hardly affects the optical properties of the surface-bound porphyrin moieties. In other words, the excited triplet state of porphyrin, through which singlet oxygen is generated, is not quenched by the superparamagnetic species in close proximity.

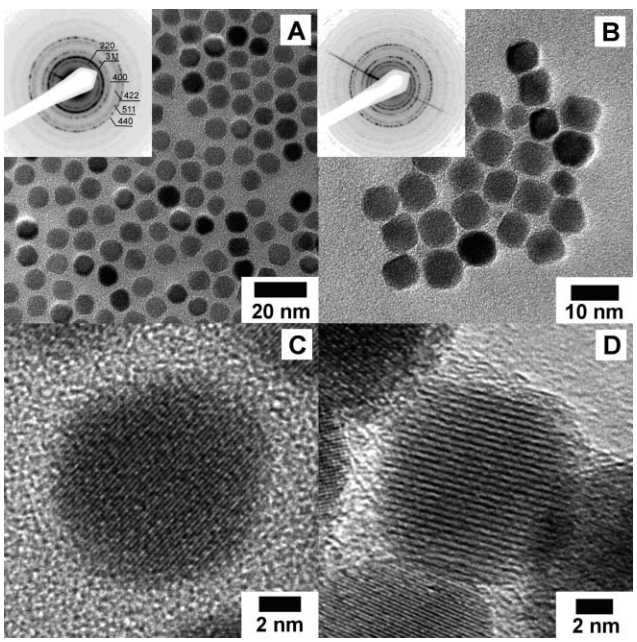

Fig. 1 TEM images of the nanoparticles of (A) Fe_3O_4 and (B) Fe_3O_4-porphyrin (**5**) (inset: SAED patterns); HRTEM images of the nanoparticles of (C) Fe_3O_4 and (D) Fe_3O_4-porphyrin (**5**).

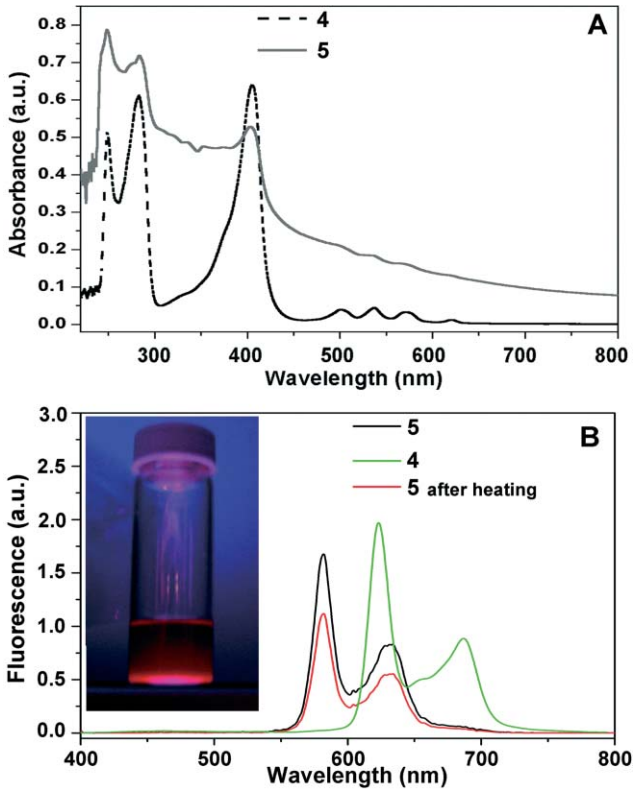

Fig. 2 (A) UV-vis spectra of **4** and **5** and (B) fluorescent spectra (λ_{ex} = 400 nm) of **4**, **5** and **5** after boiling for 30 minutes in H_2O/MeOH (inset: fluorescent image of **5** at λ_{ex} = 365 nm).

We also tested the thermal stability of **5**. As shown in Fig. 2B, after **5** was boiled in a water–methanol solution for 30 min, the fluorescent spectrum of **5** remained unaffected, suggesting that **4** remains surface-bound on the nanoparticles. This result indicates that **5** tolerates thermal treatment, which makes it an eligible candidate for HT.

Before being used as a potential bimodal anticancer agent, this molecular conjugate of porphyrin and magnetite nanoparticles should be able to enter cells. To test if **5** meets this prerequisite, we used cancer cell line HeLa to perform cellular uptake experiments for **5**. The HeLa cells were incubated with the nanoparticles (**5**) at 37 °C for 5 hours without showing observable dark toxicity. After the cells were first washed with PBS buffer three times, to remove residual nanoparticles in solution, the cells were observed under a fluorescence microscope. Being excited by yellow light (545–580 nm), **5** exhibits red emission (~610 nm). As shown in Fig. 3D,

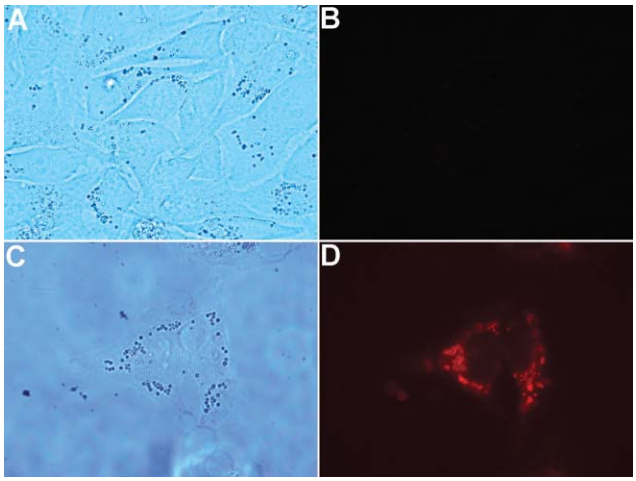

Fig. 3 Phase (A, C) and fluorescence (B, D) microscope images of HeLa cells before and after uptaking **5** intracellularly. Normal HeLa cells without **5** were observed as the control (A, B). After incubating with **5** for 5 h, HeLa cells, which were cultured on a slide, were washed with PBS buffer 3 times and then observed with an Olympus BX41 microscope at $\times 1000$ magnification (C, D). The fluorescence excitation wavelength ranges from 545 nm to 580 nm, and the emission wavelength ranges from 610 nm to infrared.

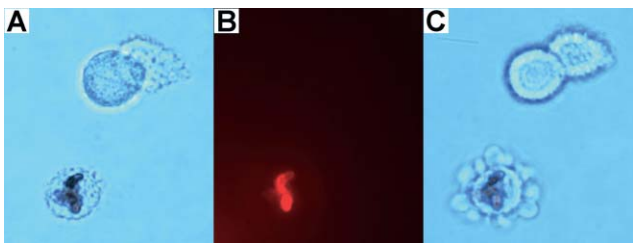

Fig. 4 Phase (A, C) and fluorescence (B) microscope images of cells uptaking **5** intracellularly. The cells were incubated with **5** for 24 h, then trypsinized, and observed as described in Fig. 3. Within 10 minutes, apoptosis could be observed surrounding the cells with **5**, while the cells nearby without nanoparticles survive the irradiation.

the nanoparticles of **5** are uptaken by the HeLa cells, likely as the result of endocytosis when the aggregates of **5** reach a certain size ($\sim$700 nm in this case).[14] Though it still remains to verify whether the porphyrins on the surface of the nanoparticles facilitate the endocytosis, it is clear that significant amounts of **5** can be uptaken by the HeLa cells. After being uptaken, the aggregates of **5** locate exclusively in the cytoplasm (Fig. 3D; the specific distribution also indicated that the nanoparticles of **5** were not absorbed outside the cell membrane), which is consistent with the intracellular location of other soluble porphyrin derivatives that are used as PDT agents.[5]

When exposed to yellow light with excitation wavelength (545–580 nm) for a short period of time (10 minutes), the cell that contains **5** exhibited a significant change of morphology (Fig. 4): the round cell changed to an irregular shape and sprouted out multiple small buds around the surface of the cell, suggesting the cell undergoes apoptosis. For the cells without the uptaken **5**, the same irradiation led to little change in their behaviors and morphology. This result clearly and qualitatively demonstrates the phototoxicity of **5**.

In conclusion, we have developed a simple, general, and robust strategy to construct the molecular conjugates of magnetic nanoparticles and porphyrin derivatives, which already meets several essential requirements of PDT and HT. This methodology should lead to a variety of bimodal conjugates like **5** for further investigations in PDT and HT as well as for other applications in the emerging field of nanomedicine.

The support by RGC (Hong Kong), DuPont Asia and European Young Faculty Grant, and HIA (HKUST) is acknowledged.

Notes and references

1 *Anticancer Agents: Frontiers in Cancer Chemotherapy*, ed. I. Ojima, G. D. Vite and K. H. Altmann, American Chemical Society, Washington DC, 2001.
2 C. Streffer, P. Vaupel and G. M. Hahn, *Biological Basis of Oncologic Thermotherapy*, Springer, Berlin, 1990.
3 A. Jordan, R. Scholz, P. Wust, H. Fahling and R. Felix, *J. Magn. Magn. Mater.*, 1999, **201**, 413.
4 K. S. Sellins and J. J. Cohen, *Radiat. Res.*, 1991, **126**, 88; J. J. Fairbairn, M. W. Khan, K. J. Ward, B. W. Loveridge, D. W. Fairbairn and K. L. O'Neill, *Cancer Lett. (Shannon, Irel.)*, 1995, **89**, 183; B. V. Harmon, Y. S. Takano, C. M. Winterford and G. C. Gobe, *Int. J. Radiat. Biol.*, 1991, **59**, 489; Y. S. Takano, B. V. Harmon and J. F. R. Kerr, *J. Pathol.*, 1991, **163**, 329.
5 *Photodynamic Therapy*, ed. D. Kessel, SPIE Optical Engineering Press, Bellingham, Washinton, 1993.
6 E. D. Sternberg and D. Dolphin, *Tetrahedron*, 54, 4151; M. R. Detty, S. L. Gibson and S. J. Wagner, *J. Med. Chem.*, 2004, **47**, 3897.
7 D. Kessel, Y. Luo, Y. Q. Deng and C. K. Chang, *Photochem. Photobiol.*, 1997, **65**, 422; R. K. Pandey, G. Zheng, D. A. Lee, T. J. Dougherty and K. M. Smith, *J. Mol. Recognit.*, 1996, **9**, 118; G. Zheng, W. R. Potter, S. H. Camacho, J. R. Missert, G. S. Wang, D. A. Bellnier, B. W. Henderson, M. A. J. Rodgers, T. J. Dougherty and R. K. Pandey, *J. Med. Chem.*, 2001, **44**, 1540; N. K. Mak, T. W. Kok, R. N. S. Wong, S. W. Lam, Y. K. Lau, W. N. Leung, N. H. Cheung, D. P. Huang, L. L. Yeung and C. K. Chang, *J. Biomed. Sci. (Basel)*, 2003, **10**, 418.
8 T. Rajh, L. X. Chen, K. Lukas, T. Liu, M. C. Thurnauer and D. M. Tiede, *J. Phys. Chem. B*, 2002, **106**, 10543; T. Rajh, Z. Saponjic, J. Liu, N. M. Dimitrijevic, N. F. Scherer, M. Vega-Arroyo, P. Zapol, L. A. Curtiss and M. C. Thurnauer, *Nano Lett.*, 2004, **4**, 1017; H. W. Gu, Z. M. Yang, J. H. Gao, C. K. Chang and B. Xu, *J. Am. Chem. Soc.*, 2005, **127**, 34.
9 C. J. Xu, K. M. Xu, H. W. Gu, H. Liu, R. K. Zheng, X. X. Zhang, Z. H. Guo and B. Xu, *J. Am. Chem. Soc.*, 2004, **126**, 9938.
10 S. Sun and H. Zheng, *J. Am. Chem. Soc.*, 2002, **124**, 8204.
11 H. Yu, M. Chen, P. M. Rice, S. X. Wang, R. L. White and S. Sun, *Nano Lett.*, 2005, **5**, 379; S. J. Park, S. Kim, S. Lee, Z. G. Khim, K. Char and T. Hyeon, *J. Am. Chem. Soc.*, 2000, **122**, 8581; J. Park, K. J. An, Y. S. Hwang, J. G. Park, H. J. Noh, J. Y. Kim, J. H. Park, N. M. Hwang and T. Hyeon, *Nat. Mater.*, 2004, **3**, 891; T. Hyeon, S. S. Lee, J. Park, Y. Chung and H. Bin Na, *J. Am. Chem. Soc.*, 2001, **123**, 12798; D. Rabelo, E. C. D. Lima, A. C. Reis, W. C. Nunes, M. A. Novak, V. K. Garg, A. C. Oliveira and P. C. Morais, *Nano Lett.*, 2001, **1**, 105; D. H. Zhang, Z. Q. Liu, S. Han, C. Li, B. Lei, M. P. Stewart, J. M. Tour and C. W. Zhou, *Nano Lett.*, 2004, **4**, 2151.
12 B. Ward, P. M. Callahan, R. Young, G. T. Babcock and C. K. Chang, *J. Am. Chem. Soc.*, 1983, **105**, 634; B. Ward, C.-B. Wang and C. K. Chang, *J. Am. Chem. Soc.*, 1981, **103**, 5236.
13 O. Q. Munro and H. M. Marques, *Inorg. Chem.*, 1996, **35**, 3768.
14 S. Stolnik, L. Illum and S. S. Davis, *Adv. Drug Delivery Rev.*, 1995, **16**, 195.

